applied sciences

MDPI

Article

Design and Experiment of an Electric Control Spiral-Pushing Feed Mechanism for Field Fertilizer Applicator

Guoqiang Dun [1,*,†], Xingpeng Wu [2,*,†], Xinxin Ji [1] and Yuhan Wei [2]

[1] Intelligent Agricultural Machinery Equipment Engineering Laboratory, Harbin Cambridge University, Harbin 150069, China; jixinxin270@163.com
[2] College of Mechanical and Electrical Engineering, Northeast Forestry University, Harbin 150040, China; weiyuhan_0820@163.com
* Correspondence: dunguoqiangpaper@163.com (G.D.); wxp13941934871@163.com (X.W.)
† These authors contributed equally to this work.

Abstract: Due to the unique structural characteristics of the traditional spiral fertilizer applicator, the instantaneous filling coefficient cannot be determined, which is not conducive to achieving precise control of the fertilizer discharge rate. Therefore, a spiral-pushing fertilizer applicator has been designed. By using a structure of variable diameter and variable spiral pitch to squeeze fertilizer gradually, precise control of the fertilizer discharge is achieved. The study analyzes the effects of screw pitch, screw diameter, and rotational speed on the filling coefficient; it uses spiral pitch elongation percentage, spiral diameter elongation percentage, and rotational speed as experimental factors, and filling coefficient and particle axial velocity coefficient as experimental indicators. Through quadratic orthogonal rotation combination design experiments, the fertilizer discharge performance of the spiral-pushing fertilizer applicator was optimized. The experimental results indicate that for the filling coefficient, x_1x_2 has an extremely significant impact, while for the axial velocity coefficient of particles, x_1 and x_3 have an extremely significant impact. When the rotational speed x_3 is 30 r/min, the optimized spiral pitch elongation percentage x_1 is 189.82–200%, the spiral diameter elongation percentage x_2 is 102.75–106.76, the filling coefficient is greater than 95%, and the particle axial velocity coefficient is less than 10%, achieving the best fertilizer discharge performance. An electrically controlled fertilizer discharge system was also designed, and bench tests were conducted on it. The results show that the average deviation between the fertilizer discharge performance of the spiral-pushing fertilizer applicator driven by the electrically controlled fertilizer discharge system and the preset value is 2.14%. This proves that, when the fertilizer demand changes, the fertilizer discharge flow can be adjusted through the electrically controlled fertilizer discharge system to achieve precise fertilization. This study provides a reference for the design of spiral fertilizer applicators.

Keywords: fertilizer discharge applicator; precise fertilization; filling coefficient; structural optimization; electrically controlled fertilizer discharge

check for updates

Citation: Dun, G.; Wu, X.; Ji, X.; Wei, Y. Design and Experiment of an Electric Control Spiral-Pushing Feed Mechanism for Field Fertilizer Applicator. *Appl. Sci.* **2023**, *13*, 12628. https://doi.org/10.3390/app132312628

Academic Editors: Jesús Montero Martínez and Jorge Cervera Gascó

Received: 27 August 2023
Revised: 11 November 2023
Accepted: 13 November 2023
Published: 23 November 2023

1. Introduction

Currently, fertilization is often used to increase crop yield, but the excessive application of fertilizers can easily cause crop lodging, environmental pollution, and resource waste. Excessive application can reduce crop yield [1–3]. The spiral fertilizer applicator is widely used in agricultural production, with advantages such as a simple structure, convenient installation, and adjustable fertilizer discharge. However, its fertilizer discharge accuracy is low, and its fertilizer discharge effect is poor. In recent years, scholars have conducted much research to improve the fertilization precision of spiral fertilizer applicators.

Dong Xiaowei [4] et al. designed a vertical spiral rice deep-side fertilizing device. Through simulation experiments and bench tests, it was determined that the best fertilization effect was achieved with a rotational speed of 190 r/min, a diameter of 22 mm, and a

forward speed of 0.45 m/s. Guoqiang Dun [5] et al. designed an oblique opening spiral fertilizer apparatus to improve the uniformity of fertilizer discharge through the oblique opening outlet method. Through bench tests, they determined that the precision of the oblique opening spiral fertilizer apparatus was better than that of the traditional spiral fertilizer apparatus. Mingda Peng [6] et al. designed a dual-directional spiral fertilizer applicator. They conducted simulation experiments with screw diameter, rotational speed, and pitch as experimental factors, and average fertilizer discharge uniformity as an experimental indicator. The results showed that when the structural parameters were a diameter of 90.1669 mm, a pitch of 59.7407 mm, and a rotational speed of 53.8944 r/min, the average fertilizer discharge uniformity reached 92.0670%. Mengqiang Zhang [7] et al. analyzed the causes of uneven fertilizer discharge from the spiral fertilizer applicator. They optimized it to determine that at a rotational speed at 47.6 r/min, a diameter of 90 mm, and a pitch of 60 mm, the uniformity of fertilizer discharge reached 19.05%, indicating a relatively good fertilizer discharge effect. Huibin Zhu [8] et al. designed a non-axis spiral fertilizer delivery device, which determined, through simulation and field experiments, that with a spiral blade radius of 12.8 mm, a pitch of 24.5 mm, and a rotational speed of 319 r/min, the fertilization accuracy error and coefficient of variation in fertilizer uniformity were 1.87% and 2.52%, respectively. Xiantao Zha [9] et al. studied and designed a blocking wheel-type screw fertilizer distributor. Through discrete element simulation, the coefficient of variation in fertilizer uniformity was optimized to less than 20% when the diameter was 17 mm, the pitch was 45 mm, and the outlet distance was 40 mm. The correctness of the simulation experiment was demonstrated through bench tests. The above research proves that, due to the structural characteristics of the spiral fertilizer applicator, fertilizer particles cannot maintain a fixed filling coefficient in the applicator cavity, making it impossible to calculate the fertilizer discharge flow rate accurately. Therefore, this article proposes the design of a spiral-pushing fertilizer applicator to increase and fix the filling coefficient by gradually reducing the amount of fertilizer discharged in a single circle, in order to accurately calculate the fertilizer discharge flow through rotation speed and achieve precise fertilization.

This article analyzes the problem of the filling coefficient in the spiral fertilizer applicator and improves the design of its spiral structure of the fertilizer applicator, thus leading to the design of a spiral-pushing fertilizer apparatus. We optimize the parameters that affect fertilizer discharge accuracy through a combination of EDEM simulation and quadratic orthogonal rotation combination design experiments. Using 3D rapid prototyping technology, a spiral-pushing fertilizer applicator was manufactured for bench verification, and an electrically controlled fertilizer discharge system was designed. The purpose of accurately controlling the fertilizer discharge flow rate through rotational speed has been achieved to provide a reference for the improved design of spiral fertilizer applicators.

2. Materials and Methods

2.1. Analysis of Fertilizer Discharge Characteristics

Due to the unique fertilizer discharge characteristics of the spiral fertilizer discharge applicator [10,11] as the spiral blade rotates, the spiral blade and the fertilizer outlet undergo periodic opening and closing changes. After the spiral rotation of the fertilizer discharge pushes the fertilizer to the outlet, the fertilizer shows a periodic downward trend with the spiral rotation, leading to fluctuations in the fertilizer discharge process. Due to the accumulation characteristics of fertilizer particles and the characteristics of the spiral blade structure, these particles often cannot fill the spiral cavity, resulting in certain gaps. The ratio of the volume of fertilizer particles in an equal-length space segment to the volume of the spiral cavity is the filling coefficient of the spiral fertilizer applicator. The stability of the filling coefficient directly affects the stability and uniformity of the spiral fertilizer feeder's discharge. When the structure of the spiral fertilizer applicator and the physical characteristics of fertilizer particles are fixed, the filling coefficient is greatly affected by the rotational speed [12].

As shown in Figure 1, the trend of filling coefficient change under different rotational speeds was analyzed using discrete element simulation, and the results are shown in Figure 2. Analysis shows that the filling coefficient is lower with a low rotational speed, and as the rotational speed increases, the filling coefficient also increases, approaching 100% after 120 r/min.

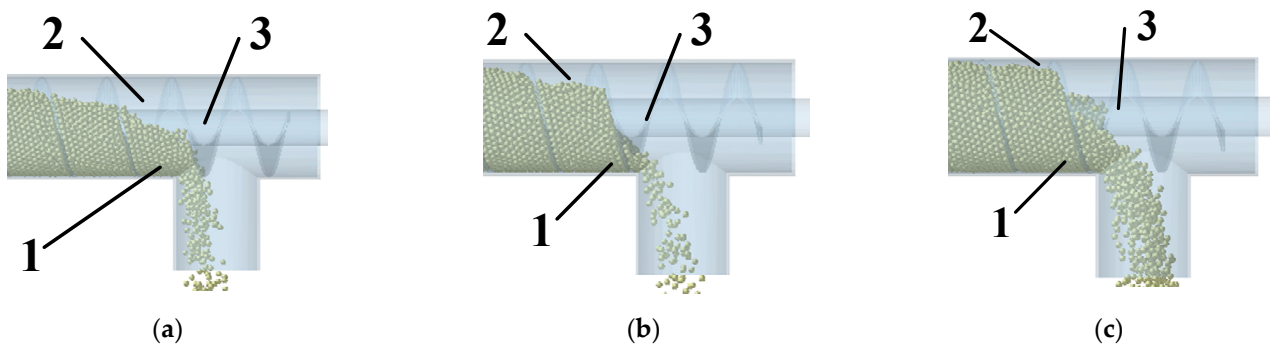

Figure 1. Trend of filling state changes when rotational speed changes: (**a**) Low rotational speed state; (**b**) Medium rotational speed state; (**c**) High rotational speed state: 1. Fertilizer particle volume, 2. Remaining cavity volume, 3. Spiral blade.

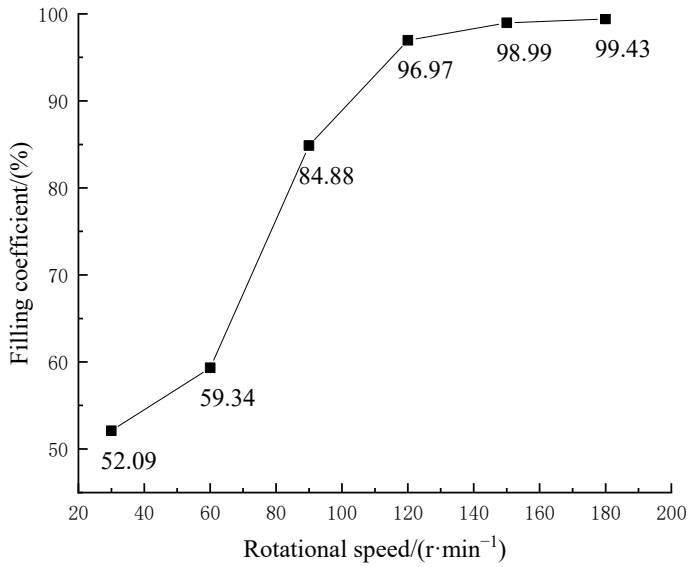

Figure 2. Filling coefficient variation curve.

2.2. Analysis of the Movement Status of Fertilizer Particles

To analyze why the spiral cavity cannot be filled when the speed of fertilizer particles is low, the movement status of fertilizer particles is analyzed as shown in Figure 3.

In Figure 3, D is the spiral diameter, mm; d is the spiral inner diameter, mm; d_1 is the distance between the particles at point O and the axis, mm; b is the thickness of the spiral blade, mm; S is the spiral pitch, mm; F_t is the axial force acting on the fertilizer particles, N; F_r is the normal phase thrust on the particle, N; F is the combined force on the particles, N; F_w is the tangential friction force, N; F_q is the circumferential component force on the particle, N; β is the spiral rise angle at the position of the particle, °; γ is the friction angle of particles on the spiral surface, °; V_t is the axial velocity of particles; V_r is the absolute velocity of particles (without considering friction); V is the absolute velocity of particles (considering frictional force); V_q is the tangential velocity of particles; V_w is the circumferential velocity of the particles.

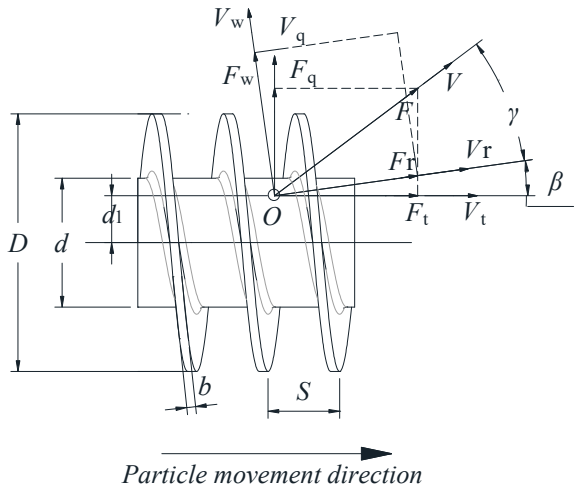

Figure 3. Characteristics of particle motion in the spiral fertilizer applicator cavity.

The circumferential and axial forces acting on the particles at point O are:

$$F_q = F\sin(\beta + \gamma) \tag{1}$$

$$F_t = F\cos(\beta + \gamma) \tag{2}$$

The spiral rise angle of particles at point O is:

$$\tan\beta = S/\pi d_1 \tag{3}$$

The friction angle between the particle and the spiral surface at point O is:

$$\gamma = \arctan\mu_1 \tag{4}$$

In the formula, μ_1 is the friction coefficient between the spiral surface and the particles.

Using Equations (1) to (4), it can be determined the magnitude of the spiral rise angle at the particle's position varies with its distance from the axis. When the friction angle on the spiral blade is fixed, the axial and circumferential forces on the particles vary with the size of the spiral rise angle [13–15]. The particle motion velocity at point O was analyzed to determine the particles' circumferential and axial motion velocities.

The circumferential velocity of particles at point O is:

$$V_w = n\pi r \tag{5}$$

The absolute velocity of particles without considering friction is:

$$V_r = V_w \sin\beta \tag{6}$$

The absolute velocity of particles when considering the frictional force is:

$$V = \frac{V_r}{\cos\gamma} \tag{7}$$

The higher the axial velocity of particles, the faster the axial conveying speed in the spiral cavity and the stronger the fertilizer discharge capacity. When the circumferential velocity is high, the rotation of the spiral blade mainly plays a starring role in the particles. Therefore, analyzing the axial and circumferential velocities of particles reveals that:

$$V_t = V\cos(\beta + \gamma) = \frac{n\pi r\sin\beta}{\cos\gamma}\cos(\beta + \gamma) \tag{8}$$

$$V_q = V\sin(\beta+\gamma) = \frac{n\pi r\sin\beta}{\cos\gamma}\sin(\beta+\gamma) \tag{9}$$

Combining Equations (8) to (9), it can be seen that the axial and circumferential forces on particles are mainly affected by the rotational speed n, spiral pitch S, and spiral diameter D. Therefore, the structural size and rotational speed of the spiral blade are calculated.

2.3. Structural Size Analysis

The amount of fertilizer discharged per unit of time via the spiral fertilizer applicator is the fertilizer discharge flow rate, mainly determined by the amount of single-circle fertilizer discharged and the rotational speed of the spiral fertilizer applicator [16]. The fertilizer discharge flow rate needs to be adjusted based on the fertilizer demand of crops.

Taking the demand for corn mid-tillage fertilization as an example, after consulting relevant literature and agronomic requirements [17,18], it is determined that the forward speed v_x is 3 m/s, the width T of the operation ridge is 0.6 m, and the fertilizer application rate R per hectare is 375kg/hm^2. According to Equation (10), the required limit fertilizer discharge Q is 67.5 g/s.

$$Q = \frac{RTv_x}{10} \tag{10}$$

In the formula: Q is the limit fertilizer discharge, g/s; R is the amount of fertilizer applied per hectare, kg/hm^2; T is the width of the homework ridge, m; v_x is the forward speed, m/s.

From Equations (11) to (12), it can be seen that when the filling coefficient μ and particle volume mass ρ are fixed, the single-circle fertilizer discharge is mainly influenced by parameters such as the thickness b of the spiral blade, spiral diameter D, spiral inner diameter d, and spiral pitch S. We determine the thickness b of the spiral blade as 2 mm, and calculate the spiral diameter D, spiral inner diameter d, and screw pitch S using Equations (13) to (15) [13,19].

$$q = \left[\frac{\pi(D^2-d^2)S}{4} - b\frac{D-d}{2}L_p\right]]\rho\mu \tag{11}$$

$$L_p = \sqrt{[\pi(D+d)/2]^2 + S^2} \tag{12}$$

$$D \geq K2.5\left(\frac{Q}{\mu\rho C}\right) \tag{13}$$

$$d = (0.2 \sim 0.35D) \tag{14}$$

$$S = (0.5 \sim 0.9D) \tag{15}$$

In the formula: q is the single-circle fertilizer discharge amount of the spiral fertilizer applicator, g; L_p is the average length of the screw teeth, mm; μ is the filling coefficient of the spiral fertilizer applicator, with a value of 1; ρ is the volumetric mass of the material, in t/m^3, taken as 0.948 t/m^3 [20]; Q is the required maximum fertilizer discharge, t/h; C is the inclination coefficient of the spiral fertilizer applicator, as the spiral fertilizer applicator is horizontally placed, the inclination coefficient is taken as 1; K is the comprehensive coefficient of the material, with a value of 0.045 [21].

According to Equation (13), the minimum required spiral diameter D is 26.11 mm. Referring to the existing spiral fertilizer applicator, the range of spiral diameter D is determined to be 40–50 mm, and the inner diameter d is calculated to be 10 mm through Equations (14) to (15), with the spiral pitch S range of 20–40 mm.

The rotational speed is the decisive factor affecting the fertilizer discharge flow rate, and the fertilizer discharge flow rate, fertilizer discharge uniformity, and filling coefficient all increase with the increase in rotational speed [22].

However, excessive rotational speed can cause the fertilizer particles to roll in the spiral cavity, causing the spiral blades to lose their axial propulsion function. Therefore, it is necessary to calculate the limit rotational speed of the spiral fertilizer feeder to ensure normal fertilizer discharge.

The relationship between the maximum centrifugal force of particles and their gravity during regular operation of the screw fertilizer applicator is:

$$m\omega_{\max}^2 r \leq mg \tag{16}$$

$$\frac{2\pi n_{\max}}{60} \leq \sqrt{\frac{g}{r}} \tag{17}$$

When the fertilizer particles are different, the relationship equation is:

$$\frac{\pi n_{\max}}{30} \leq K\sqrt{\frac{g}{r}} \tag{18}$$

$$n_{\max} = \frac{30K}{\pi}\sqrt{\frac{g}{r}} = \frac{30K}{\pi}\sqrt{\frac{2g}{D}} \tag{19}$$

At $A = 30K\sqrt{2g}/\pi$, the maximum rotational speed of the spiral blade is:

$$n_{\max} \leq \frac{A}{\sqrt{D}} \tag{20}$$

In the formula, r is the radius of the spiral blade, and based on the calculation, the spiral diameter range is obtained, taking r as 0.025 m; m is the mass of fertilizer particles, kg; g is the acceleration of gravity, m/s^2; $\omega_{\max}$ is the maximum angular velocity of the spiral blade, rad/s; A is the comprehensive characteristic coefficient of the material, with a value of A = 50 [11]. According to Equation (20), the limit rotational speed $n_{\max}$ of the screw fertilizer applicator is calculated to be 223.61 r/min.

$$Q_{\max} = \left[\frac{\pi\left(D^2 - d^2\right)S}{4} - b\frac{D-d}{2}L_p\right]\rho\mu n_{\max} \tag{21}$$

In the formula, $Q_{\max}$ is the limit fertilizer discharge, g/s.

Based on the minimum structural dimensions of the spiral fertilizer applicator: the spiral diameter D is 40 mm, spiral inner diameter d is 10 mm, spiral pitch S is 20 mm, and spiral blade thickness b is 2 mm, the maximum fertilizer discharge flow $Q_{\max}$ is calculated as 74.65 g/s through Equation (21). The required fertilizer discharge flow rate Q is 67.5 g/s, which meets the design requirement of a 375 kg/hm^2 fertilizer demand during corn mid-tillage fertilization.

2.4. Improved Design of Spiral Fertilizer Discharge Applicator

This article proposes an incremental improvement design for the spiral blade's spiral diameter and pitch to increase the filling coefficient of the screw fertilizer discharge applicator. As shown in Figure 4, the spiral blade is divided into three steps from the fertilizer outlet to the fertilizer inlet, the fertilizer discharge section Q_3, the extrusion fertilizer section Q_2, and the accumulation fertilizer section Q_1.

To fix the single-circle fertilizer discharge quality q, we refer to the structural size parameter range of the spiral fertilizer applicator. The screw diameter D_3 of the fixed fertilizer discharge section is 40 mm, and the screw pitch S_3 size is 20 mm. The maximum spiral diameter D_1 and spiral pitch S_1 of the spiral in the accumulation fertilizer section are designed to be 50 mm and 40 mm, respectively.

During operation, the fertilizer particles in the fertilizer applicator cavity are squeezed from the extrusion fertilizer section to the fully filled state, and the filling coefficient is kept

stable to ensure that the fertilizer discharge flow rate is calculated through the rotational speed and single-circle fertilizer discharge quality.

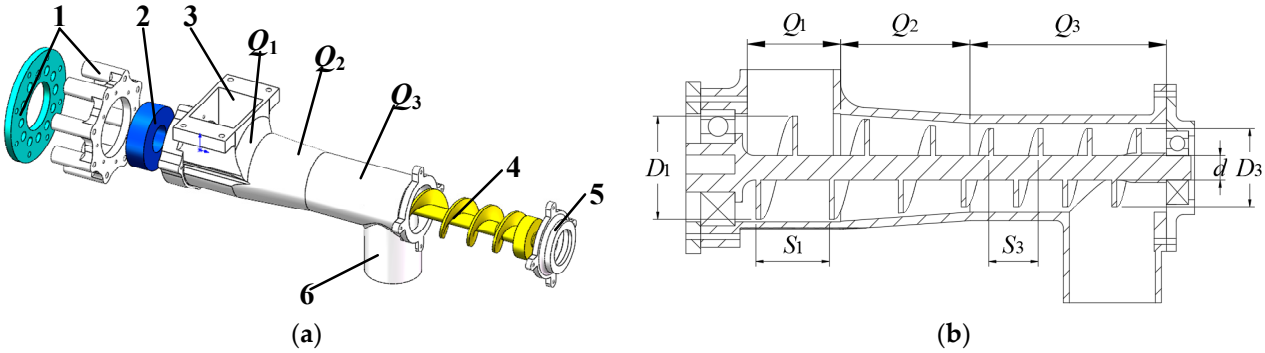

Figure 4. Improvement design of spiral-pushing fertilizer applicator: (**a**) Structural model of spiral-pushing fertilizer applicator; (**b**) Spiral blade structure: 1. Motor connection frame, 2. Bearings, 3. Fertilizer inlet, 4. Spiral blade, 5. End cover, 6. Fertilizer outlet.

2.5. Simulation Model Establishment and Parameter Setting

To analyze the fertilizer discharge performance of the spiral-pushing fertilizer applicator under different structural sizes, this paper simulates the fertilizer discharge process through EDEM discrete element simulation experiments [23,24]. As shown in Figure 5, we constructed the fertilizer particle factory in the spiral fertilizer applicator feeder box, generating 5000 fertilizer particles per second after the start of the experiment, totaling 10,000 fertilizer particles. After the particles naturally fall along the z-axis into the spiral fertilizer applicator for 0.5 s, the spiral blade begins to rotate. The rotational speed range is 30–220 r/min, and the forward speed of the fertilizer applicator is set to 0.5 m/s. We also established a monitoring area in the fertilizer discharge section to monitor the particle quality and axial velocity coefficient.

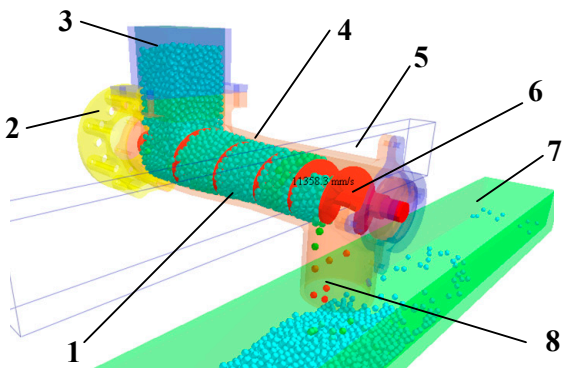

Figure 5. Simulation model of spiral-pushing fertilizer applicator: 1. Fertilizer particles, 2. Motor connection frame, 3. Fertilizer particle factory, 4. Spiral-pushing fertilizer applicator shell, 5. Monitoring area, 6. Spiral blade, 7. Fertilizer collection tank, 8. Fertilizer outlet.

After consulting relevant literature [25], it was determined that the built-in model Hertz Mindlin (no slip) of EDEM is the contact model between particles and the spiral fertilizer applicator. We randomly selected 100 fertilizer particles from the urea fertilizer produced by Jinmei Hengsheng Chemical Co., Ltd., in Xuzhou City, Jiangsu Province, China, and measured their diameters in three dimensions: length, width, and thickness.

The measurement result shows that the average equivalent diameter of one hundred particles is 2.05 mm, the sphericity is 96.12%, and the standard deviation of radius is 0.199 mm. They were regarded as spherical particles with a diameter of 2.05 mm and determined as fertilizer particles for simulation experiments. The material of the spiral-pushing fertilizer applicator was selected as PLA plastic. Relevant literature [26] was

consulted to determine the parameters related to fertilizer particles and PLA plastic. The results are shown in Table 1.

Table 1. Discrete element simulation parameter settings.

Parameter	Fertilizer Particles	Spiral Fertilizer Applicator
Poisson ratio	0.25	0.43
Shear modulus (Pa)	1.0×10^7	1.3×10^9
Density (kg·m^3)	1345	1240
Static friction coefficient–fertilizer particles	0.4	0.5
Rolling friction coefficient–fertilizer particles	0.01	0.01
Restitution coefficient–fertilizer particles	0.6	0.5

2.6. Evaluation Method for Fertilizer Discharge Performance

This article selects the filling coefficient μ and particle axial velocity coefficient y_1 as experimental evaluation indicators. Figure 6 shows the time-series state diagram of the simulation process of the spiral-pushing fertilizer applicator. Analysis shows that the fertilizer particles remain filled after being squeezed in the extrusion fertilizer section of the spiral-pushing fertilizer applicator.

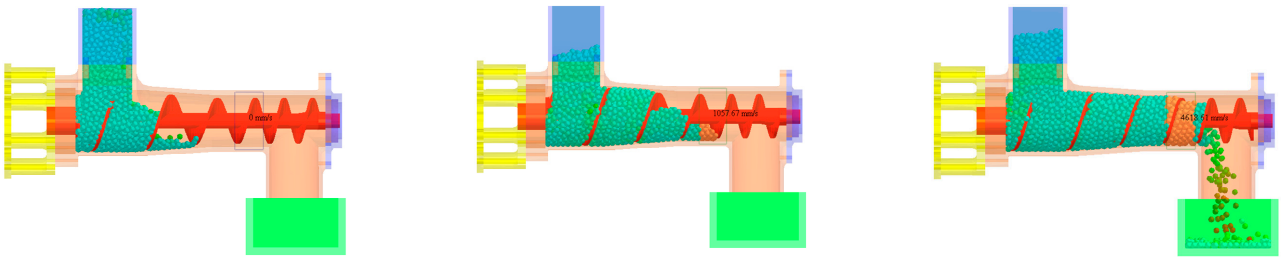

(**a**) (**b**) (**c**)

Figure 6. Simulation process of spiral-pushing fertilizer applicator: (**a**) 1 s; (**b**) 2.5 s; (**c**) 5 s.

The following steps are undertaken to determine the variation trend of the fertilizer particle quality and axial velocity in the monitoring area of the fertilizer discharge section. After the spiral-pushing fertilizer applicator stabilizes the fertilizer discharge, the total particle mass and particle axial velocity data at each monitoring point within 1 s of the monitoring area are randomly intercepted, and the mean is taken as the mean of the total particle mass m_{average} and the mean of the total particle velocity v_{average}. The filling coefficient μ can be calculated using Equation (22) based on m_{average} and the cavity volume I.

$$\mu = \frac{m_{\text{average}}/\rho}{I} \tag{22}$$

In the formula, m_{average} is the average total mass of particles in the monitoring area, g; I is the volume of the cavity space, mm^3.

After being squeezed, the particles' speed is affected by the rotational speed and the extrusion and propulsion of other fertilizer particles behind them. To accurately analyze the influence of the structure of the spiral blade on the particle velocity, the particle axial velocity coefficient y_1 was calculated using Equations (23) to (24).

The smaller the particle axial velocity coefficient y_1, the faster the axial velocity of the particles in the applicator cavity, indicating that the particle flow state is better. The higher the filling coefficient μ of the fertilizer particles in the applicator cavity, the more controllable the fertilizer discharge flow rate, but it is prone to blockage of the fertilizer particles. Therefore, increasing the filling coefficient μ while keeping the particle axial

velocity coefficient y_1 as small as possible ensures the fertilizer discharge effect of the spiral-pushing fertilizer applicator.

$$v_{speed} = S_{\max}\frac{n}{60} \tag{23}$$

$$y_1 = 1 - \frac{v_{speed} - v_{\text{average}}}{v_{speed}} \tag{24}$$

In the formula, v_{speed} is the displacement distance of the spiral blade, mm/s; $S_{\max}$ is the spiral pitch of the accumulation fertilizer section, mm; v_{average} is the average total velocity of fertilizer particles, mm/s.

2.7. Range of Test Factors

Based on the parameter calculation results, it is determined that the spiral pitch of the fertilizer discharge section is 20 mm, and the spiral diameter is 40 mm. The maximum spiral pitch of the accumulation fertilizer section is 40 mm, and the maximum spiral diameter is 50 mm. We determine the spiral pitch elongation percentage x_1 to be within a range of 100~200%, the spiral diameter elongation percentage x_2 to be within a range of 100~125%, and the rotational speed x_3 to be within a range of 30~220 r/min. We conduct a quadratic orthogonal rotation combination design experiment, and the coding table of the experimental factors is shown in Table 2. The quadratic orthogonal rotation combination design experiment was designed based on the coding table of the experimental factors, with a total of twenty-three groups of experiments designed. Each set of tests was repeated three times, and the average value was taken as the result.

Table 2. Factor-level coding table.

Code	Factor		
	x_1/%	x_2/%	x_3/r·Min^{-1}
1.682	200.00	125.00	220
1	179.73	119.93	181.49
0	150.00	112.50	125.00
−1	120.27	105.07	68.51
−1.682	100.00	100.00	30.00

3. Results

3.1. Analysis of Test Results

To determine the fertilizer discharge effect of the spiral-pushing fertilizer applicator with different parameters in the simulation state, quadratic orthogonal rotation combination design experiments were used to analyze the simulation results comprehensively. The test and regression analysis results are shown in Table 3, Table 4, and Table 5, respectively.

The results from Table 4 show that the filling coefficient regression model is significant, with a specific value of (p = 0.0159 < 0.05), and its regression model mismatch term is not significant, with a specific value of (p = 0.3360 > 0.001). For the filling coefficient test indicators, x_1x_2 has an extremely significant impact, with x_1, x_2, x_1x_2, and ${x_2}^2$ having a significant impact, while the other factors have no significant impact.

The results from Table 5 show that the regression model for the particle axial velocity coefficient is extremely significant (p = 0.0019 < 0.001), and its regression model mismatch term is not significant (p = 0.3193 > 0.001). For the particle axial velocity coefficient test indicators, x_1 and x_3 have an extremely significant impact, while the other factors have no significant impact.

Excluding insignificant factors from the regression equation, the regression equations for the filling coefficient and particle axial velocity coefficient are:

$$\begin{cases} \mu = 429.973 + 1.557x_1 - 7.760x_2 + 0.039x_3 \\ -0.022x_1x_2 + 0.003{x_1}^2 + 0.047{x_2}^2 \\ y_1 = 59.95 - 0.27x_1 + 0.07x_3 \end{cases} \quad (25)$$

Table 3. Schemes and results of tests.

Code	Test Factor			Test Indexes	
	x_1/%	x_2/%	x_3/r·Min^{-1}	y_1/%	μ/%
1	120.27	105.07	68.51	29.02	94.54
2	179.73	105.07	68.51	13.81	97.55
3	120.27	119.93	68.51	39.26	99.32
4	179.73	119.93	68.51	12.60	77.86
5	120.27	105.07	181.49	39.57	96.21
6	179.73	105.07	181.49	20.03	99.66
7	120.27	119.93	181.49	41.45	99.39
8	179.73	119.93	181.49	25.50	88.69
9	100.00	112.50	125.00	34.25	95.12
10	200.00	112.50	125.00	14.12	86.93
11	150.00	100.00	125.00	26.20	96.12
12	150.00	125.00	125.00	25.01	87.36
13	150.00	112.50	30.00	17.96	77.71
14	150.00	112.50	220.00	29.89	87.06
15	150.00	112.50	125.00	28.15	85.52
16	150.00	112.50	125.00	29.27	86.93
17	150.00	112.50	125.00	25.55	80.32
18	150.00	112.50	125.00	27.71	87.71
19	150.00	112.50	125.00	31.26	83.65
20	150.00	112.50	125.00	32.72	88.95
21	150.00	112.50	125.00	35.81	92.27
22	150.00	112.50	125.00	27.28	89.68
23	150.00	112.50	125.00	20.95	94.31

Table 4. Filling coefficient analysis table.

Filling Coefficient μ/%					
Source of Variance	**Square SUM**	**Degree of Freedom**	**Mean Square**	***F*-Value**	***p*-Value**
Model	697.14	9	77.46	3.74	0.0159
x_1	114.10	1	114.10	5.50	0.0355
x_2	102.60	1	102.60	4.95	0.0445
x_3	67.69	1	67.69	3.26	0.0940
x_1x_2	186.44	1	186.44	8.99	0.0103
x_1x_3	15.68	1	15.68	0.76	0.4003
x_2x_3	6.34	1	6.34	0.31	0.5898
${x_1}^2$	88.63	1	88.63	4.27	0.0592
${x_2}^2$	108.61	1	108.61	5.24	0.0395
${x_3}^2$	7.63	1	7.63	0.37	0.5546
Residual	269.58	13	20.74		
Misfit term	123.31	5	24.66	1.35	0.3360
Pure error	146.27	8	18.28		
Total variation	966.72	22			

Table 5. Analysis of variance of the particle axial velocity coefficient.

Particle Axial Velocity Coefficient y_1/%					
Source of Variance	**Square SUM**	**Degree of Freedom**	**Mean Square**	***F*-Value**	***p*-Value**
Model	1163.52	9	129.28	6.10	0.0019
x_1	905.67	1	905.67	42.74	<0.0001
x_2	15.14	1	15.14	0.71	0.4132
x_3	197.42	1	197.42	9.32	0.0093
x_1x_2	7.72	1	7.72	0.36	0.5564
x_1x_3	5.09	1	5.09	0.24	0.6323
x_2x_3	0.35	1	0.35	0.02	0.8993
${x_1}^2$	13.45	1	13.45	0.63	0.4398
${x_2}^2$	2.78	1	2.78	0.13	0.7231
${x_3}^2$	16.28	1	16.28	0.77	0.3967
Residual	275.45	13	21.19		
Misfit term	128.59	5	25.72	1.40	0.3193
Pure error	146.86	8	18.36		
Total variation	1438.97	22			

3.2. Analysis of Experimental Factors

To analyze the trend in the influence of experimental factors on the filling coefficient and particle axial velocity coefficient, response surface plots and single-factor plots were used for analysis.

As shown in Figure 7, when the diameter elongation percentage is fixed, the filling coefficient shows a significant decrease and then a slight increase with the reduction in the spiral pitch elongation percentage at the lower part of the diameter elongation percentage and a significant increase at the higher part in the diameter elongation percentage. When the spiral pitch elongation percentage is fixed, the filling coefficient decreases with the decrease in the diameter elongation percentage, showing a trend of first decreasing and then slightly increasing when the spiral pitch elongation percentage is low and a significant increasing trend when the spiral diameter elongation percentage is high.

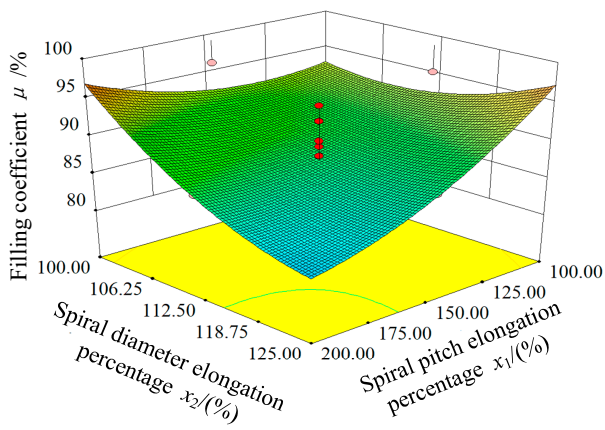

Figure 7. Response surface graph of the filling coefficient.

The red dots in Figures 8 and 9 represent the experimental values of repeated experiments, and the lines serve as the relationship curve between the experimental factors and the experimental indicators. As shown in Figures 8 and 9, the particle axial velocity coefficient shows a decreasing trend as the spiral pitch elongation percentage increases. In contrast, as the rotational speed increases, the particle axial velocity coefficient shows an increasing trend.

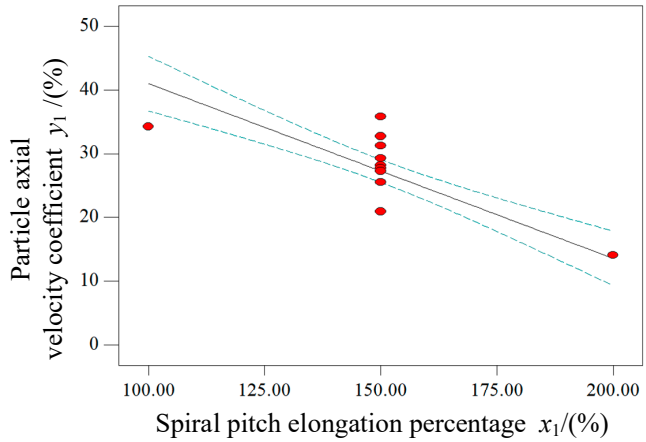

Figure 8. Analysis of the influence of spiral pitch elongation percentage on the particle axial velocity coefficient.

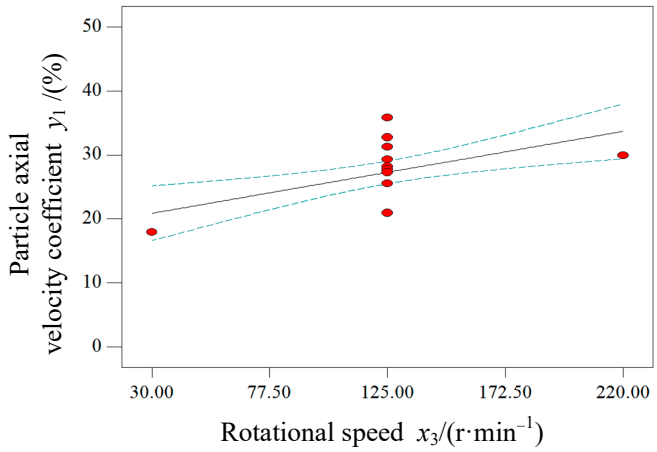

Figure 9. Analysis of the influence of rotational speed on the particle axial velocity coefficient.

3.3. Parameter Optimization Results

The lower the particle axial velocity coefficient, the faster the axial velocity of fertilizer particles, and the less likely it is to block the fertilizer applicator cavity. The higher the filling coefficient, the more stable the filling coefficient. Based on practical work experience in the market, the particle axial velocity coefficient should be less than 10%, and the filling coefficient should be more significant than 95%. The results from Figure 1 show that the filling coefficient of the spiral-pushing fertilizer applicator is lower at low rotational speeds. Therefore, the fixed spiral-pushing fertilizer applicator rotational speed is 30 r/min, and x_1 and x_2 are optimized. The results are shown in Figure 10.

The yellow shaded area in Figure 6 is the optimal combination area for x_1 and x_2. The results from Figure 10 show that the yellow shaded area in the figure represents the optimal combination of the spiral pitch elongation percentage x_1 and the spiral diameter elongation percentage x_2. When the spiral pitch elongation percentage is within a range of 189.82–200%, and the spiral diameter elongation percentage is within a range of 102.75–106.76%, the filling coefficient is more significant than 95%, and the particle axial velocity coefficient is less than 10%. When selecting the spiral pitch elongation percentage of 190% within the optimization interval, the spiral diameter elongation percentage is 105%. The accumulation fertilizer section's calculated spiral pitch and diameter are 38 mm and 42 mm. Through simulation verification, it was determined that the filling coefficient of the optimized spiral-pushing fertilizer applicator was 97.24%, and the particle axial velocity coefficient was 7.61%, which met an optimization range and proved the correctness of the parameter optimization.

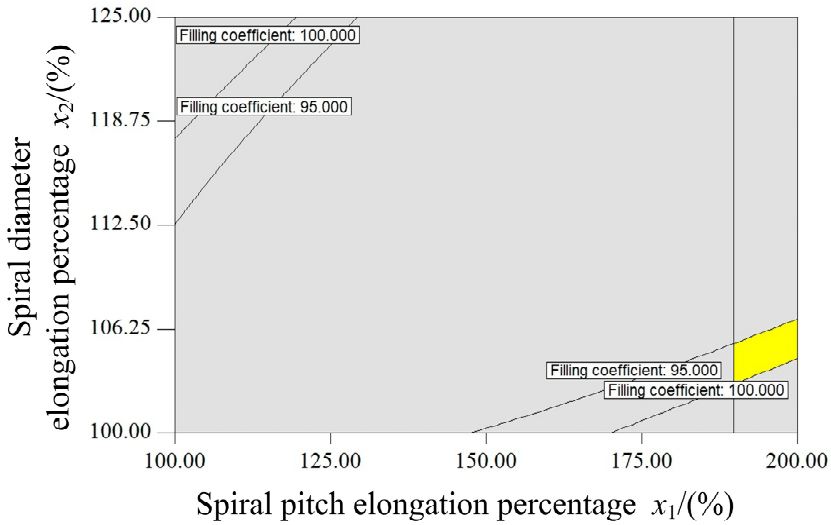

Figure 10. Parameter optimization results.

3.4. Validation Test Results

In order to verify the fertilizer discharge effect of the optimized spiral-pushing fertilizer applicator (OSPFA), based on the optimal results of optimization, it was determined that the accumulation fertilizer section pitch of the spiral-pushing fertilizer applicator was 38 mm, with the diameter of 42 mm, and the fertilizer discharge section was 20 mm, with a diameter of 40 mm. The urea fertilizer produced via Jinmei Hengsheng Chemical Co., Ltd., in Xuzhou City, Jiangsu Province, China, was selected as the experimental fertilizer granules.

As shown in Figure 11, a prototype of the optimized spiral-pushing fertilizer applicator (OSPFA) and the traditional spiral fertilizer applicator (TSFA) were processed using 3D rapid printing technology, and comparative experiments were conducted in the Intelligent Agricultural Machinery Equipment Engineering Laboratory of Harbin Cambridge University for verification.

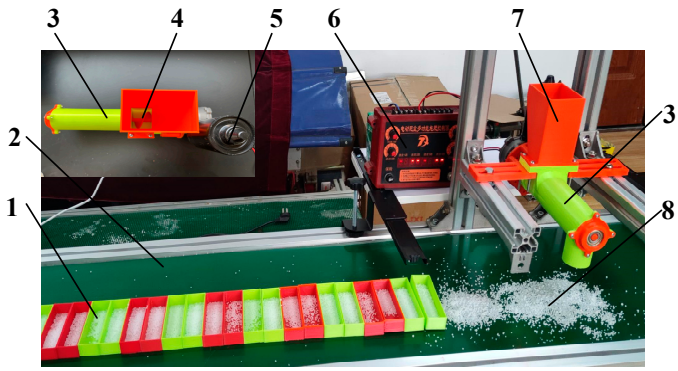

Figure 11. Bench verification test: 1. Fertilizer collection box, 2. Conveyor belt, 3. Spiral-pushing fertilizer applicator, 4. Spiral blade, 5. Drive motor, 6. Rotational speed controller, 7. Fertilizer box, 8. Fertilizer particles.

The rotational speed of the spiral blade was set to 30, 60, 90, 120, 150, 180, and 210 r/min, and the forward speed of the conveyor belt was set to 0.1 m/s. Selecting the fertilizer discharge flow rate as the experimental indicator, the quality of fertilizer in the fertilizer box was measured using a Japanese GX-8K electronic scale. After the spiral-pushing fertilizer applicator stabilizes the fertilizer discharge, we collected the number of fertilizer boxes within a distance range of five seconds of the conveyor belt, calculated their average fertilizer discharge flow rate per second, and repeated the experiment three times to take their average. The experimental results are shown in Figure 12.

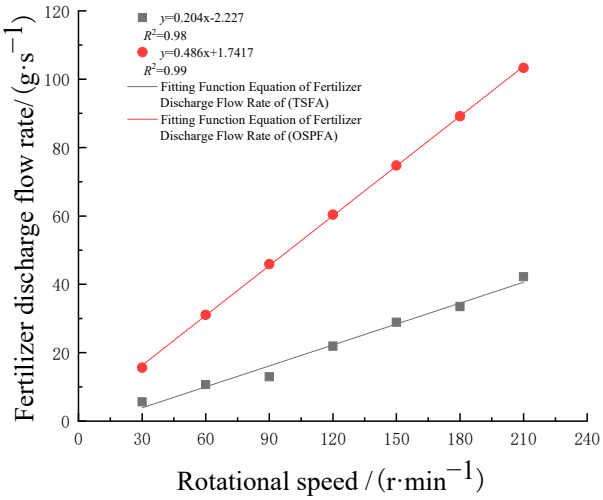

Figure 12. Comparison chart of fertilizer discharge flow rate.

The results from Figure 12 show that the fitting function equation of the fertilizer discharge flow rate of the spiral-pushing fertilizer applicator is $y = 0.486x + 1.7417$, and R^2 is 0.99. The fitting function equation for the discharge flow rate of a traditional spiral fertilizer applicator is $y = 0.204x - 2.227$, and R^2 is 0.98. This proves that the linear relationship between the changing trend in the fertilizer discharge flow rate of the spiral-pushing fertilizer applicator is better, and the fitting effect is better than that of the traditional screw fertilizer applicator. Thus, it can precisely adjust its fertilizer discharge flow rate by adjusting the rotational speed.

To achieve the design goal of automatically and accurately adjusting the rotational speed according to the fertilizer demand of crops to adjust the spiral-pushing fertilizer applicator fertilizer discharge flow rate, this article designs an electrically controlled fertilizer discharge system with a built-in driving function based on the fertilizer discharge flow equation $y = 0.486x + 1.7417$. When the fertilizer demand of crops changes, the rotation speed of the spiral-pushing fertilizer applicator can vary according to the change in fertilizer demand.

To verify the fertilizer discharge performance of the electrically controlled fertilizer discharge system, as shown in Figure 13, the electrically controlled fertilizer discharge system was verified in bench tests. We then repeated the experiment thrice at rotational speeds of 37, 49, 85, 134, 161, 179, and 205 r/min, and took the average as the test result. We then compared the results with the preset fertilizer discharge flow rate, as shown in Figure 14. Analysis shows that the average deviation between the spiral-pushing fertilizer applicator controlled is implemented through an electrically controlled fertilizer discharge system. The preset value is 2.14%, which meets the design requirements.

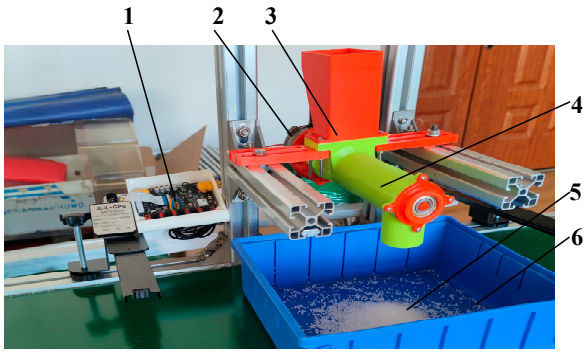

Figure 13. Verification test of electric control spiral-pushing fertilizer applicator on the bench: 1. Electrically controlled fertilizer discharge system, 2. Drive motor, 3. Fertilizer box, 4. Spiral-pushing fertilizer applicator, 5. Fertilizer particles, 6. Fertilizer collection box.

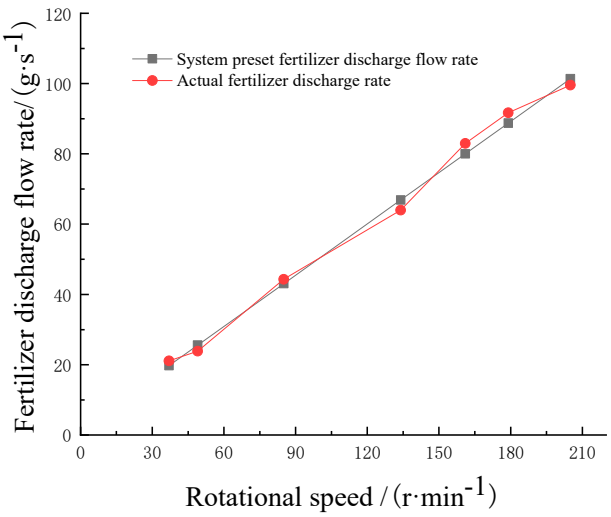

Figure 14. Comparison curve of fertilizer discharge flow rate of electrically controlled fertilizer discharge device.

4. Discussion

(1) In the actual operation process of the traditional spiral fertilizer applicator, the filling coefficient does not change linearly with the rotational speed change. Therefore, to achieve precise fertilizer discharge, this article designs a spiral-pushing fertilizer applicator, which mainly changes the pitch and diameter of the existing spiral fertilizer applicator, so that its instantaneous filling coefficient is in a fixed state of full filling. Based on the movement trend for fertilizer particles in the spiral cavity, the main factors affecting the movement characteristics of fertilizer particles were determined to be the spiral diameter, pitch, and rotational speed. Through EDEM, a simulation model of the spiral-pushing fertilizer applicator was established to analyze the fertilizer discharge status during the fertilizer discharge process of the spiral-pushing fertilizer applicator. A quadratic orthogonal rotation combination design experiment was conducted with the filling coefficient and particle axial velocity coefficient as experimental indicators and the spiral pitch elongation percentage, spiral diameter elongation percentage, and rotational speed as experimental factors.

(2) The experimental results show that the spiral pitch elongation percentage and spiral diameter elongation percentage have a significant impact on the filling coefficient. In contrast, the spiral pitch elongation percentage and rotational speed have a significant effect on the particle axial velocity coefficient. Based on the experimental results, the parameters of the spiral-pushing fertilizer applicator were optimized. The results showed that when the spiral pitch elongation percentage was 189.82–200%, the spiral diameter elongation percentage was 102.75–106.76%, and the rotational speed was 30 r/min, the filling coefficient was 97.24%, and the particle axial velocity coefficient was 7.61%. The traditional spiral fertilizer applicator has a filling coefficient of 52.09% at a rotational speed of 30 r/min. This indicates that under a low rotational speed, the spiral-pushing fertilizer applicator has a high filling coefficient and good fluidity of fertilizer particles in the spiral cavity.

(3) To verify the correctness of the optimization results, a comparative test was conducted through bench tests on the spiral-pushing fertilizer applicator and the spiral fertilizer applicator. The results show that the fitting equation R^2 = 0.99 for the spiral-pushing fertilizer applicator flow rate and the fitting function equation R^2 = 0.98 for the traditional spiral fertilizer applicator discharge flow rate. This proves that the spiral-pushing fertilizer applicator discharge performance was significantly better than the traditional spiral fertilizer applicator discharge during bench tests. It was feasible to achieve precise fertilizer discharge by improving the spiral cavity filling co-

efficient. Based on the discharge flow curve of the spiral-pushing fertilizer applicator y = 0.486x + 1.7417, an electrically controlled fertilizer discharge system was designed and tested on a bench. The bench test results showed that the spiral-pushing fertilizer applicator controlled by the electrically controlled fertilizer discharge system had a high precision in fertilizer discharge, and the rotational speed could accurately adjust the fertilizer discharge flow to meet the fertilizer demand in the fields.

Author Contributions: G.D. and X.W. designed the research. X.W., X.J. and Y.W. participated in the measurements and data analysis, and X.W. wrote the first draft of the manuscript. G.D. and X.W. revised and edited the final version of the manuscript. G.D. was responsible for funding acquisition. All authors have read and agreed to the published version of the manuscript.

Funding: This research was funded by Heilongjiang Province Natural Science Foundation of China, grant number LH2023E025; Harbin Cambridge University Key Scientific Research Application Research Project, grant number JQZKY2022021.

Institutional Review Board Statement: Not applicable.

Informed Consent Statement: Not applicable.

Data Availability Statement: Data are contained within the article.

Acknowledgments: The author would like to thank their school and Heilongjiang Ruilong Innovation Technology Co., Ltd., for their funding of this project. All authors sincerely appreciate the support and assistance.

Conflicts of Interest: The authors declare that this study received funding from Heilongjiang Ruilong Innovation Technology Co., Ltd. The funder was not involved in the study design, collection, analysis, interpretation of data, the writing of this article or the decision to submit it for publication.

References

1. Tan, S.; Xie, D.; Ni, J.; Chen, F.; Ni, C.; Shao, J.; Zhu, D.; Wang, S.; Lei, P.; Zhao, G.; et al. Characteristics and Influencing Factors of Chemical Fertilizer and Pesticide Applications by Farmers in Hilly and Mountainous Areas of Southwest, China. *Ecol. Indic.* **2022**, *143*, 109346. [CrossRef]
2. Zhao, J.; Wang, X.; Tian, H.; Lu, Y.; Guo, C.; Liu, H. A Fertilizer Discharge Detection System Based on Point Cloud Data and an Efficient Volume Conversion Algorithm. *Comput. Electron. Agric.* **2021**, *185*, 106131. [CrossRef]
3. He, Y.; Zhao, X.; Li, C.; Dou, H.; Li, S.; Wang, X. Research Status and Analysis on Fertilization Technology of Corn Topdressing Machinery. *J. Agric. Mech. Res.* **2021**, *43*, 1–9. [CrossRef]
4. Dong, X. *Mechanism and Parameters of Vertical Spiral Rice Deep-Side Fertilizing Device*; Heilongjiang Bayi Agricultural University: Daqing, China, 2019.
5. Dun, G.; Wu, X.; Ji, X.; Ji, W.; Ma, H. Optimization Design and Experiment of Qblique Opening Spiral Precision Control Fertilizer Apparatus. Trans. *Chin. Soc. Agric. Mach.* **2023**, *54*, 167–174.
6. Peng, M.; Zhang, Z.; Zhang, W.; Huang, H.; Zhang, G.; Liu, W.; Wu, X.; Zhang, J. Design and Optimization of Sugarcane Spiral Fertilizer Applicator Based on Response Surface Methodology and Artificial Neural Networks. *Processes* **2023**, *11*, 2881. [CrossRef]
7. Zhang, M.; Tang, Y.; Zhang, H.; Lan, H.; Niu, H. Parameter Optimization of Spiral Fertilizer Applicator Based on Artificial Neural Network. *Sustainability* **2023**, *15*, 1744. [CrossRef]
8. Zhu, H.; Wu, X.; Bai, L.; Wang, M.; Lei, F.; Fang, Y. Design and Experiment of Shaftless Spirals Fertilizer Discharging and Fertilizer Delivery Device of No-tilliage Planters. *Trans. Chin. Soc.Agric. Mach.* **2023**, 1–14.
9. Agriculture. Structural Optimization and Performance Evaluation of Blocking Wheel-Type Screw Fertilizer Distributor. Available online: https://www.mdpi.com/2077-0472/11/3/248 (accessed on 22 July 2023).
10. Xiao, W.; Liao, Y.; Shan, Y.; Li, M.; Wang, L.; Liao, Q. Design and Experiment of Quad-screw Double-row Fertilizer Apparatus for Rape Seeding Machine. *Trans. Chin. Soc.Agric. Mach.* **2021**, *52*, 68–77. [CrossRef]
11. Yang, W.; Fang, L.; Luo, X.; Li, H.; Ye, Y.; Liang, Z. Experimental study of the effects of discharge port parameters on the fertilizing performance for fertilizer distribution apparatus with screw. *Trans. Chin. Soc. Agric. Eng.* **2020**, *36*, 1–8. [CrossRef]
12. Chen, X.; Luo, X.; Wang, Z.; Zhang, M.; Hu, L.; Yang, W. Design and experiment of fertilizer distribution apparatus with double-level screws. *Trans. Chin. Soc. Agric. Eng.* **2015**, *31*, 10–16. [CrossRef]
13. Qi, J.; Meng, H.; Kan, Z.; Li, C.; Li, Y. Analysis and test of feeding performance of dual-spiral cow feeding device based on EDEM. *Trans. Chin. Soc. Agric. Eng.* **2017**, *33*, 65–71. [CrossRef]
14. Zheng, K.; Liu, G.; Guo, L.; Cheng, J.; Xia, J.; Li, Y. Design and Experiment of Wide-boundary Seldom-tillage Wheat Planter with Soil-shunting Function. *Trans. Chin. Soc. Agric. Mach.* **2022**, *53*, 128–138. [CrossRef]
15. Hu, Y.; Dai, L.; Pi, Y. Theories and Calculation of the Auger–Type Conveyer. *J. Nanchang Univ. Eng. Technol.* **2000**, *4*, 29–33+91.

16. Dun, G.; Liu, W.; Wu, X.; Mao, N.; Ji, W.; Ma, H. Simulation optimization design and experiment of screw extrusion precision fertilizer ejector. *J. Jilin. Univ.* **2023**, *11*, 18. [CrossRef]
17. Zhang, H. *Effects of Density and Fertilizer Amount on Agronomic Characters and Yield of Corn Shennong T100*; Shenyang Agricultural University: Shenyang, China, 2021.
18. Li, Z. *Design and Experimental Study on Fertilizer Shovel of Fertilizer Cultivator*; Northeast Agricultural University: Haerbin, China, 2014.
19. China Academy of Agricultural Mechanization. *Agricultural Machinery Design Manual*; China Agricultural Science and Technology Press: Beijing, China, 2007; Volume 2.
20. Yu, C. *Design and Test Study of Gear Type Anti-Blocking Separated Layer Fertilization Device Based on Discrete Element Method*; Northeast Forestry University: Haerbin, China, 2021.
21. Zhang, X.; Liu, Y.; Li, L.; Tong, Z.; Yang, D.; Hou, C. Design and performance experiment of multi-segment type auger in process of organic fertilizer production. *Trans. Chin. Soc. Agric. Eng.* **2018**, *34*, 49–56.
22. Xue, Z.; Zhao, L.; Wang, F.; Wang, S.; Song, G.; Wang, G. Study on the Performance of Spiral Fertilizer Distributor Based on EDEM. *J. Agric. Mech. Res.* **2020**, *42*, 87–95. [CrossRef]
23. Dun, G.; Mao, N.; Ji, X.; Zhang, F.; Ji, W. Optimal Design and Experiment of Corn-Overlapped Strip Fertilizer Spreader. *Appl. Sci.* **2023**, *13*, 2559. [CrossRef]
24. Van Liedekerke, P.; Tijskens, E.; Dintwa, E.; Rioual, F.; Vangeyte, J.; Ramon, H. DEM Simulations of the Particle Flow on a Centrifugal Fertilizer Spreader. *Powder Technol.* **2009**, *190*, 348–360. [CrossRef]
25. Lv, H.; Yu, J.; Fu, H. Simulation of the Operation of a Fertilizer Spreader Based on an Outer Groove Wheel Using a Discrete Element Method. *Math. Comput. Model.* **2013**, *58*, 842–851. [CrossRef]
26. Dun, G.; Yu, C.; Guo, Y.; Ji, W.; Islam, K.R.; Du, J. Design and Experiment of Double-gear Type Fertilizer Apparatus. *Trans. Chin. Soc. Agric. Mach.* **2020**, *51*, 87–96. [CrossRef]